

Research Paper

Synthesis of Acetylene Black and Polyvinylidene Difluoride to Improve the Conductivity of Li-ion Nickel Manganese Cobalt Batteries

Totok Dermawan¹ ✉, Agus Sudjatno¹, Edy Yulianto², Suroso¹, Yustinus Purwamargapratala³, Budi Suhendro¹, Ign Agus Purbhadi Wirgiyanto¹

¹Department of Electro Mechanic, Indonesian Nuclear Technology Polytechnic, Sleman 55281, Indonesia

²Research Center for Advanced Materials, National Research and Innovation Agency, South Tangerang 15314, Indonesia

³National Research and Innovation Agency, Sleman 55281, Indonesia

✉ toto003@brin.go.id

🌐 <https://doi.org/10.31603/ae.12329>

Published by Automotive Laboratory of Universitas Muhammadiyah Magelang

Article Info

Submitted:

18/09/2024

Revised:

07/01/2025

Accepted:

09/01/2025

Online first:

18/01/2025

Abstract

The issue of low cathode conductivity is a significant challenge in battery development, particularly for automotive applications. The cathode plays a crucial role in Li-ion batteries, as it is responsible for transferring lithium ions during both charging and discharging processes. Therefore, this study aims to enhance the conductivity of the cathode by incorporating Acetylene Black (AB) and Polyvinylidene Difluoride (PVDF) additives. In this study, Nickel Manganese Cobalt (NMC) 811 and NMC 111 cathodes were used. These materials were formed into pellets, then made into sheets, with AB and PVDF additives added in a weight composition ratio of 85:10:5, and a coating thickness of 300 μm . The cathode conductivity was characterized using an LCR meter, while surface morphology, cross-section, EDS, and mapping of the cathode surface were analyzed with SEM. The results showed that the addition of additives increased the conductivity of NMC 111 by more than five times, from $23.27 \times 10^{-8} \text{ S.cm}^{-1}$ to $119.34 \times 10^{-8} \text{ S.cm}^{-1}$, and NMC 811 by more than twelve times, from $6.43 \times 10^{-8} \text{ S.cm}^{-1}$ to $81.79 \times 10^{-8} \text{ S.cm}^{-1}$. These findings suggest that higher particle density, improved size distribution, and smaller particle grains contribute to higher conductivity.

Keywords: NMC; Conductivity; Li-ion battery; Acetylene black; Polyvinylidene difluoride

1. Introduction

Many studies have been conducted to enhance the efficiency of electric vehicles, aiming to achieve energy-efficient and environmentally friendly transportation [1]–[4]. One crucial component currently under development is the vehicle battery, which requires an adequate and appropriate power supply [5], [6]. The battery's capacity is significantly influenced by the quality of the cathode, as this component facilitates the transfer of ions during both charging and discharging processes [7], [8].

In recent years, extensive research is focused on improving battery performance by enhancing the conductivity of the cathode. Nickel Manganese Cobalt (NMC) cathodes are

particularly notable due to their superior properties for producing high-energy batteries, making them highly suitable for practical applications [7]. Fakhruddin et al. [9] improved the cyclic and rate performance of NMC cathodes by coating cerium oxide (CeO_2) and Yalçın et al. [10] by doping NMC with Sn for energy retention. Similarly, Darjazi et al. [11] enhanced the structural stability, charge-discharge voltage, and cycle stability of NMC cathodes by doping them with MgCr. Additionally, Metal-Organic Frameworks (MOF) carbon materials have been employed to coat the surfaces of lithium battery electrodes, improving the effectiveness of electrochemical energy conversion and storage methods [12].



This work is licensed under a Creative Commons Attribution-NonCommercial 4.0 International License.

The use of Acetylene Black (AB) and Polyvinylidene Fluoride (PVDF) additives has shown significant potential for meeting the demands of large-capacity and environmentally friendly batteries [13], [14]. Therefore, the effects of cathode thickness and grain density on battery capacity as indicated by cathode conductivity, need to be further examined. Previous studies have primarily focused either on the impact of cathode thickness on battery capacity [15], [16] or on the effects of grain size and density [17], [18], but not on their combined influence.

To address this gap, this research investigates the relationship between cathode thickness and microstructures of NMC to enhance battery performance by improving the conductivity of the NMC cathode. This approach will provide a clearer understanding of how cathode thickness and microstructure affect cathode conductivity. The findings are expected to contribute to optimizing the lithium-ion transfer process during charging and discharging. The study involves adding AB and PVDF additives to NMC 811 and NMC 111 cathodes, aiming to increase the conductivity of the NMC cathode and, consequently, improve the overall performance of lithium-ion batteries.

2. Methods

In our current work, 5 grams of slurry were prepared as the material for fabricating NMC cathode sheets, as shown in [Figure 1](#). The cathode

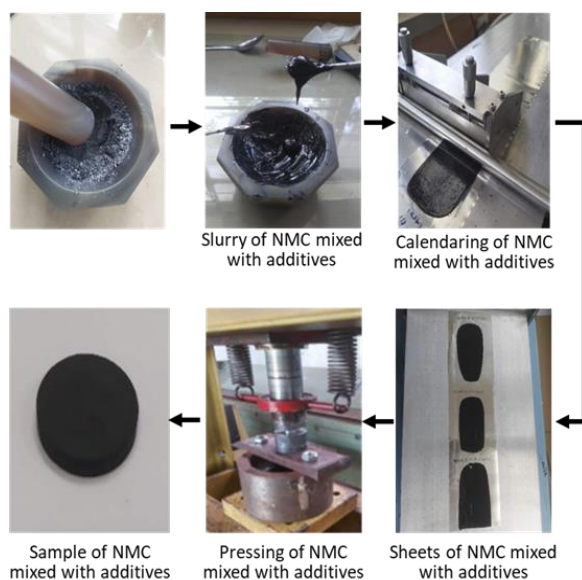


Figure 1. Research workflow for the addition of AB and PVDF additives to the NMC cathode

slurry consisted of NMC powder, AB, and PVDF in a weight ratio of 4.24 g : 0.5 g : 0.25 g, equivalent to 85%:10%:5%. The NMC, AB, and PVDF powders were ground together using an agate mortar for approximately 15 minutes until evenly mixed and free of lumps. During this process, N-Methyl-2-Pyrrolidone (NMP) solution was gradually added in small amounts, totaling approximately 8 mL, until a homogeneous slurry was obtained. The NMC cathode slurry was then coated onto an aluminum sheet, which served as the current collector, using an applicator to achieve a slurry thickness of 300 μm . The coated slurry was subsequently dried in a vacuum oven at 80 $^{\circ}\text{C}$ for 24 hours, resulting in the formation of the NMC cathode sheet.

An LCR meter is used to measure the conductivity of cathode pellets and coated cathode sheets. The powder cathodes were prepared by compacting them under a pressure of 4000 psi using a hydraulic press with a die diameter of 15 mm and a sample weight of 2 g, resulting in circular NMC samples with a diameter of 15 mm and a thickness of 1.8 mm. A Scanning Electron Microscope (SEM) was used to observe the morphology and mapping of the surface and cross-sections of the samples [19], [20].

For cross-sectional observation, NMC 811 and NMC 111 cathode sheets were prepared with a slurry thickness of 300 μm , and the top layer consisted of a 0.017 mm aluminum sheet cut to 0.015 mm. The samples were arranged in layers (sandwich structure) using carbon tape to ensure the layers remained intact during testing. The samples were placed in a standing position within the center of a mold made from PVC pipe sections with a diameter of 1 inch and a thickness of 15 mm. The sandwich structure was then embedded in resin. Afterward, the resin-embedded samples were polished using sandpaper with a progressively finer grit, ranging from 400 to 5000 mesh, and finally smoothed with an alumina suspension.

3. Results and Discussion

Morphological characterization using SEM was performed at 1,000x magnification to analyze the powder morphology of NMC 811 and NMC 111, as shown in [Figure 2a](#) and [Figure 2b](#). Both materials exhibit uniform spherical particles with varying sizes on a microscale. However, NMC 111

features relatively uniform, light-colored flake-like shapes. **Figure 3a** and **Figure 3b** depict the surface morphology of NMC powders compacted into pellets: NMC 811 (**Figure 3a**) and NMC 111 (**Figure 3b**). The pellets exhibit similar morphological features, including spherical particles with smaller flake-like particles. However, visible gaps or cavities remain between the particles, indicating areas not fully filled by the active material.

In **Figure 4a** and **Figure 4b**, differences in morphology are evident. **Figure 4a** illustrates the

surface morphology of the coating before the calendaring process, while **Figure 4b** shows the morphology after calendaring. Before calendaring, the NMC 811 and NMC 111 cathodes exhibit uneven surfaces with irregularly sized particles protruding from the surface and visible cracks evenly distributed across the variations in slurry thickness. These cracks likely result from structural changes during the drying process at 80 °C. After calendaring (**Figure 4b**), the cathode surface appears smoother, with cracks and gaps from the drying process no longer visible.

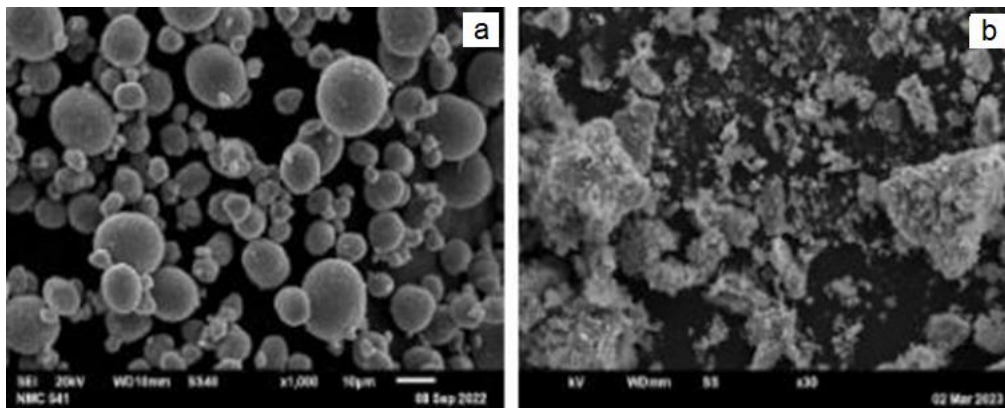


Figure 2. Powder morphology: (a) NMC 811 and (b) NMC 811

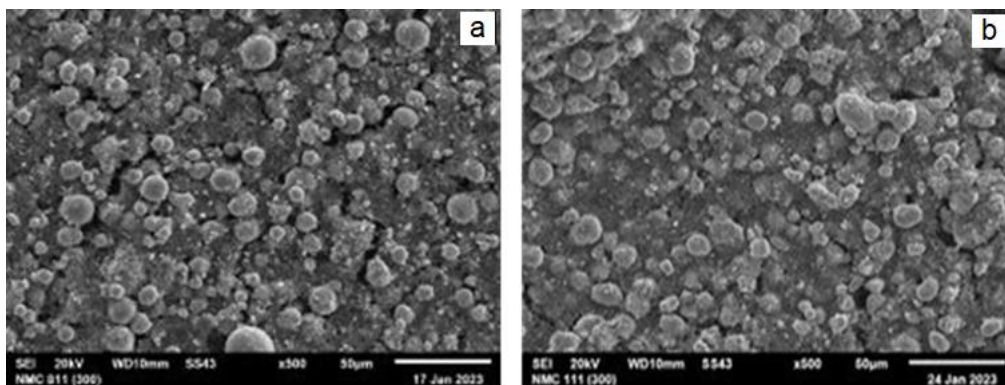


Figure 3. Surface morphology of coated NMC: (a) NMC 811 and (b) NMC 111

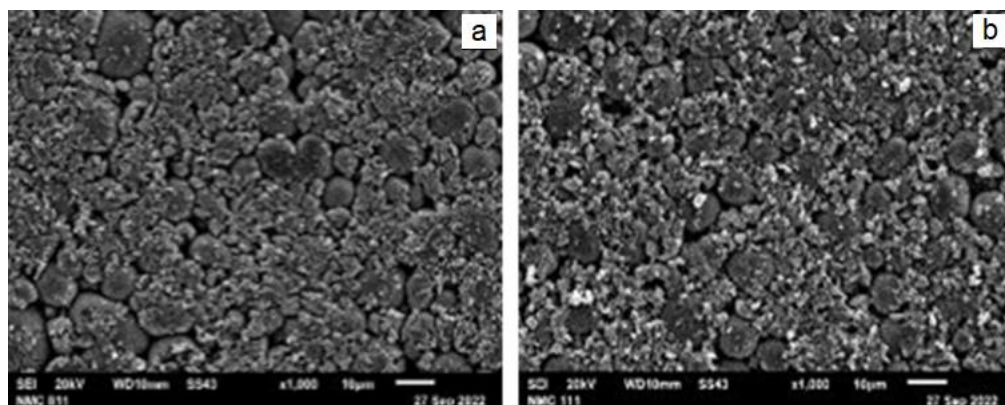


Figure 4. Surface morphology of NMC pellets: (a) NMC 811 and (b) NMC 111

The cross-sectional morphology of the NMC cathodes was also examined to observe internal structural changes due to compression. Compared to surface morphology observations, NMC 111 displays a denser structure, with smaller particle fragments filling the gaps between larger spherical particles, potentially improving conductivity. However, the surface remains relatively uneven, following the crack paths caused by sample fracturing during preparation.

SEM morphological characterization of the MNC cathode resulting from coating using the cross-section method as presented in [Figure 5a](#) and [Figure 5b](#), while [Figure 6a](#) and [Figure 6b](#) present the SEM morphology of the MNC cathode resulting from coating after the calendaring process using the cross-section method. From the two images, the difference between the cathode resulting from coating before the calendaring process and after the calendaring process is clearly visible. On the cathode resulting from coating before the calendaring process, it is very clear that the surface is uneven on almost all sides, and particles with different sizes also appear to protrude on the

surface of the coating result. The distance between one particle and another with a ball-shaped pattern also looks uneven. Meanwhile, after going through the calendaring process, the cathode surface becomes more even, and the thickness of the active material also gets smaller, this automatically has an impact on the distance between the particles that are getting closer together. [Table 1](#) presents the thickness shrinkage value after the calendaring process.

Based on [Table 1](#), the shrinkage value of the cathode sheet after going through the calendaring process decreased by an average of around 31.293 μm . It can be seen that there has been a decrease in the thickness of the coated cathode sheet of $\pm 25.867\%$. This is due to the evaporation of the solvent liquid at the same time as the drying process of the cathode sheet using an oven it affects the distance between particles and results in the thinning of the coated cathode layer. [Table 2](#) presents data on the effectiveness of the slurry thickness on the coating results on the cathode sheet.

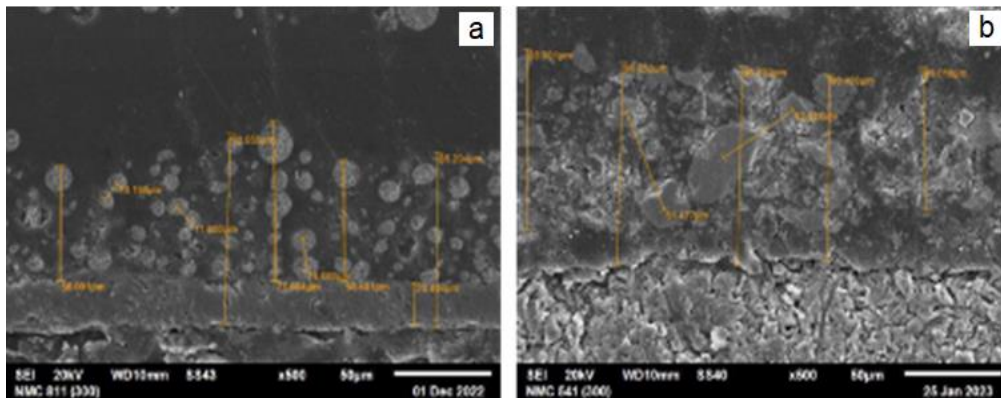


Figure 5. Cross-sectional morphology of coated NMC cathode: (a) NMC 811 and (b) NMC 111

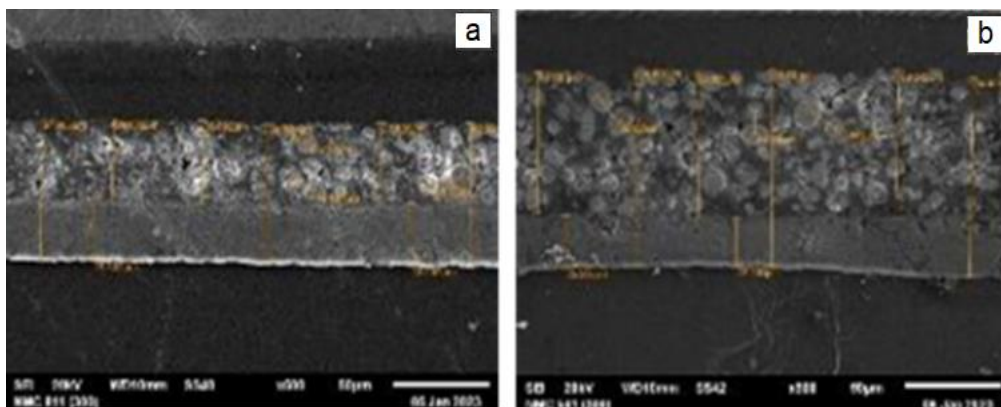


Figure 6. Cross-sectional morphology of MNC cathode after calendaring process: (a) NMC 8111 and (b) NMC 111

Table 1. Effectiveness of coated cathode

| Type of NMC | Coating Thickness (μm) | Effectiveness (%) |
|-------------|-------------------------------------|-------------------|
| 811 | 58.401 | 18.799 |
| 111 | 96.801 | 43.787 |

Table 2. Thickness shrinkage after calendaring process

| Type of NMC | Cathode Thickness (μm) | | Shrinkage (μm) |
|-------------|-------------------------------------|--------------------|-----------------------------|
| | Before callendering | After callendering | |
| 811 | 58.401 | 39.602 | 18.799 |
| 111 | 96.801 | 52.014 | 43.787 |

Energy Dispersive Spectroscopy (EDS) is used to quantitatively analyze the elemental composition of Ni, Mn, and Co materials. The results of EDS characterization, presented as graphs showing the relationship between intensity and energy, are displayed in [Figure 7a](#) and [Figure 7b](#). [Table 3](#) summarizes the elemental composition percentages for the NMC powder material. EDS characterization provides a means to compare the chemical composition percentages of the base NMC material. [Table 4](#) presents a comparison of the chemical compositions of the NMC powder material. Based on the compositional analysis using Energy Dispersive X-ray (EDX) on NMC 811 cathode powder material, the atomic composition percentages of Ni, Mn, and Co are 46.05%, 5.04%, and 6.47%, respectively. For NMC 111, the percentages are 22.05%, 20.13%, and 20.20%, respectively.

The EDS results for the coated cathode sheets, which compare the elemental composition percentages of NMC: PVDF: AB in an 85:10:5 ratio, indicate that carbon (C) is the dominant element. This dominance is due to the combination of AB and PVDF, the latter of which has a chemical composition of $(\text{CH}_2\text{-CF}_2)_n$, also known as difluoroethylene. Changes in the percentages of Ni, Mn, and Co in the coated materials, compared to the original powder, can be attributed to the addition of AB and PVDF as additives.

[Figure 8a](#) and [Figure 8b](#) illustrate the intensity-energy relationship for the EDS characterization of Ni, Mn, and Co. For the coated cathode sheets, the compositional analysis using EDX reveals the atomic percentages of Ni, Mn, Co, and C as 11.28%, 10.93%, 10.37%, and 93.44% for NMC 811, and 19.12%, 6.46%, 6.50%, and 41.04% for NMC

111. From the mapping, it is evident that the elements Ni, Mn, and Co are distributed homogeneously across each surface of the sample, as shown in [Figure 9](#). However, in [Figure 10](#), several cavities are visible. This is due to the uneven particle size distribution, which causes a slight reduction in color brightness. In contrast, [Figure 8b](#) shows a more homogeneous and denser element distribution, as smaller, flake-like particles fill the gaps between larger particles, resulting in a more even color brightness.

Previous research has shown the surface morphology of the NMC 811 cathode material. The composition of the cathode material indicates that the NMC 811 cathode was successfully synthesized with nickel content ranging from 73% to 79%, manganese from 9% to 13%, and cobalt from 10% to 13%. Lithium-ion batteries using the NMC 811 cathode demonstrate capacities of 15.09 mAh/g at 20g/L, 28.42 mAh/g at 30g/L, and 25.57 mAh/g at 40g/L [21].

A study on the synthesis and characterization of a solid electrolyte based on lithium glass $(\text{AgI})_{0.33}(\text{LiI})_{0.33}(\text{LiPO}_3)_{0.3}$ reported a conductivity value of 2.35×10^{-3} S/cm for the LIXY component at 33.33, which is higher than that of LiPO_3 , which has a conductivity of 1.24×10^{-6} to 1.24×10^{-7} S/cm [21]. Testing of active cathode materials in pellet form was conducted to facilitate the characterization process. The results of conductivity testing for the active materials NMC 811 and NMC 111 using the HIOKI 3532-50 LCR meter are presented in [Table 4](#). The conductivity measurements for the NMC 811 and NMC 111 cathode sheets, with a coating thickness of 300 μm , are shown in [Table 5](#).

Table 3. Elements content of NMC powder

| Type of NMC | Nickel (%) | Manganese (%) | Cobalt (%) |
|-------------|------------|---------------|------------|
| 811 | 46.05 | 5.04 | 6.47 |
| 111 | 22.05 | 20.13 | 20.20 |

Table 4. Elemental content of the cathode sheet

| Type of NMC | Nickel (%) | Manganese (%) | Cobalt (%) | Carbon (%) |
|-------------|------------|---------------|------------|------------|
| 811 | 11.28 | 10.93 | 10.37 | 93.44 |
| 111 | 19.12 | 6.46 | 41.04 | 41.04 |

Table 5. Conductivity of pellet NMC and cathode sheet NMC

| Type of NMC | Conductivity (S.cm ⁻¹) | |
|-------------|------------------------------------|-------------------------|
| | Pellet | Cathode Sheet |
| 811 | 6.43x10 ⁻⁸ | 81.79x10 ⁻⁸ |
| 111 | 23.27x10 ⁻⁸ | 119.34x10 ⁻⁸ |

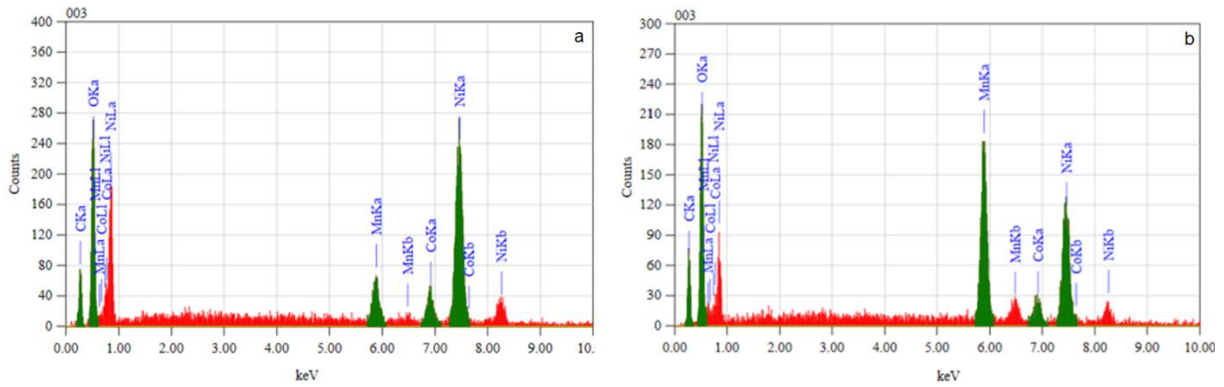


Figure 7. Relationship between intensity and energy from EDS characterization of NMC powder: (a) NMC 811 and (b) NMC 111

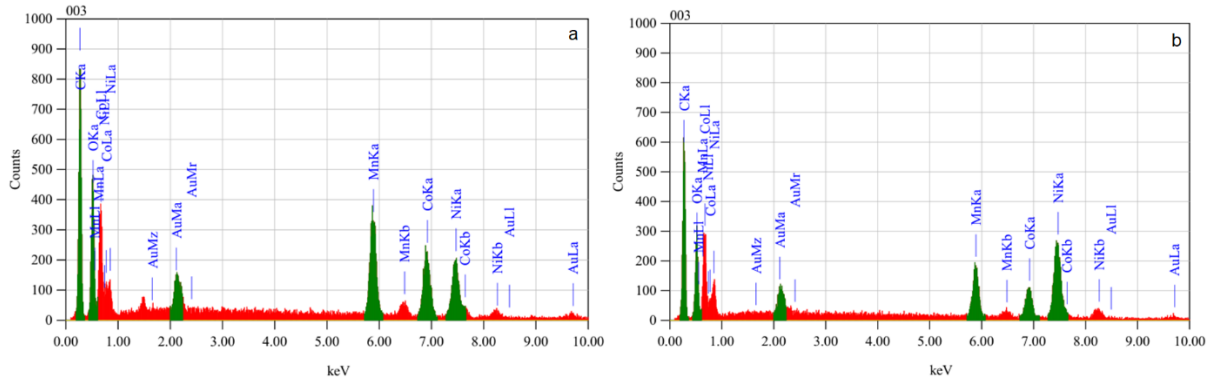


Figure 8. Relationship between intensity and energy from EDS characterization of cathode sheets: (a) NMC 811 (b) NMC 111

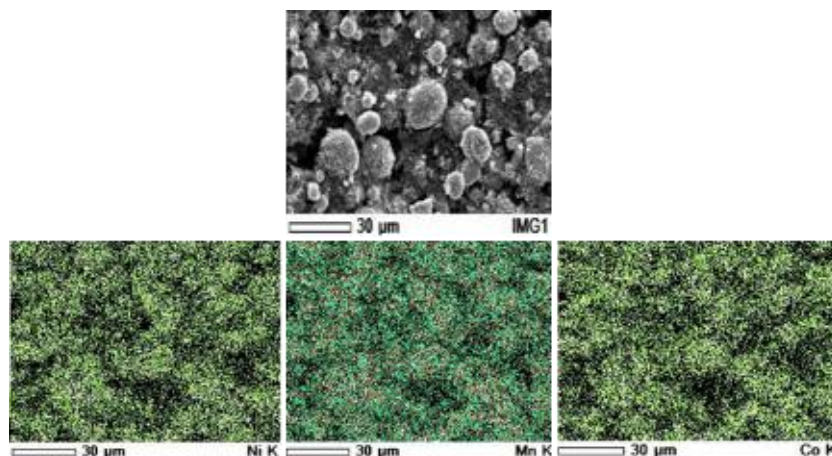


Figure 9. Mapping the surface of NMC 811 cathode

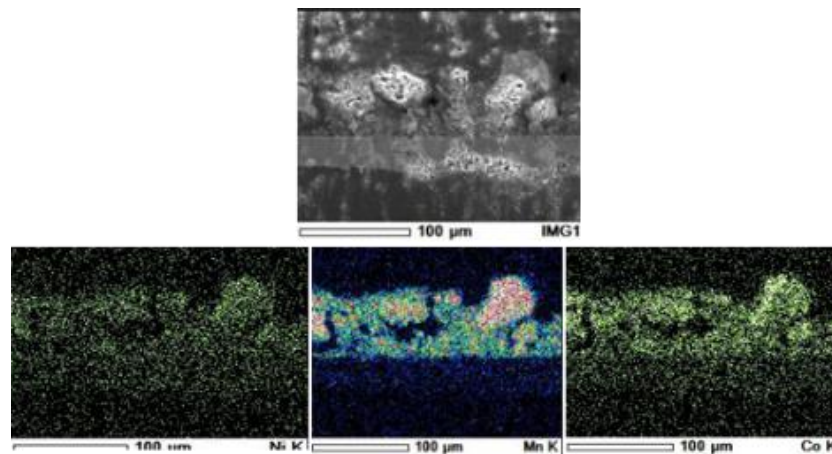


Figure 10. Mapping of cross-section sheet of NMC 111 cathode

Figure 11 and Figure 12 show the cross-sectional morphology of the NMC 811 and NMC 111 samples. In both images, the distribution of internal elements is uneven, and cavities are present in some areas, as indicated by the variation in brightness levels. This suggests the need for a calendaring process to reduce the distance between particles and decrease the thickness of the cathode, which can improve the conductivity and capacity of the battery.

Table 5 shows a difference in conductivity between the active material of the pellet cathode and the coated cathode sheet, as well as differences in compositional analysis using EDX. The pellet cathode is made from pure NMC material, while the coated cathode sheet is a composite material, combining NMC with other active materials such as Acetylene Black (AB) powder and Polyvinylidene difluoride (PVDF) in a weight ratio of 85:10:5. Despite these differences, both materials show an increase in conductivity for the cathode sheet that was successfully produced.

Mapping and morphological observations, including both surface and cross-sectional methods of the coated cathode sheet, reveal several differences before and after the calendaring process for both NMC 811 and NMC 111, such as element distribution, particle size, and density. NMC 111 has a denser structure than NMC 811, leading to a more even element distribution, which in turn increases conductivity. Conductivity measurements for the two coated NMC samples showed a value of $119.34 \times 10^{-8} \text{ S}\cdot\text{cm}^{-1}$ for NMC 811, and $81.79 \times 10^{-8} \text{ S}\cdot\text{cm}^{-1}$ for NMC 111.

Higher cathode conductivity leads to increased battery capacity [22]. Research by Yujie Song et

al. [16] shows that increasing cathode thickness enhances battery capacity. At thicknesses of 100-200 microns, the increase in cathode thickness correlates with improved conductivity, which aligns with the results of this study. For NMC 111, which has been coated, an increase in cathode thickness from 200 microns to 300 microns corresponds to an increase in conductivity from 4.13×10^{-8} to 119.34×10^{-8} . For NMC 811, the conductivity increased from 81.79×10^{-8} to 199.71×10^{-8} as the cathode thickness grew from 300 microns to 400 microns.

Research by Jihyeon Kang et al. [15] indicates that there is an optimal thickness that results in the highest conductivity. Our study also suggests that each type of cathode has an optimal thickness for maximum conductivity. This optimal thickness is influenced by the grain size and compactness of the cathode; smaller grain sizes and greater compactness result in better conductivity. These findings are consistent with research by Jelle Smekens, et al. [18] and Ruonan Yang, et al. [17].

4. Conclusion

This study aimed to determine the optimal conditions for NMC 111 and NMC 811 cathodes with AB and PVDF additives to achieve high conductivity, considering both the cathode thickness and its microstructural conditions. The results showed that cathodes with additives significantly increased conductivity—NMC 111 improved more than fivefold, from $23.27 \times 10^{-8} \text{ S}\cdot\text{cm}^{-1}$ to $119.34 \times 10^{-8} \text{ S}\cdot\text{cm}^{-1}$, and NMC 811 increased more than twelvefold, from $6.43 \times 10^{-8} \text{ S}\cdot\text{cm}^{-1}$ to $81.79 \times 10^{-8} \text{ S}\cdot\text{cm}^{-1}$. Additionally, it was found that higher particle density, better size distribution, and finer particle grains resulted in

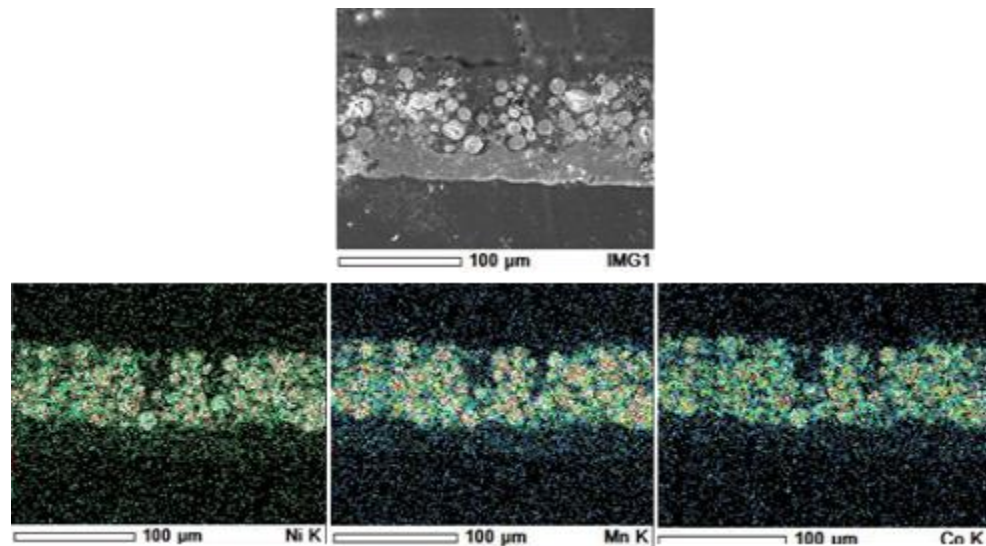


Figure 11. Mapping of cross-section of cathode sheet NMC 811

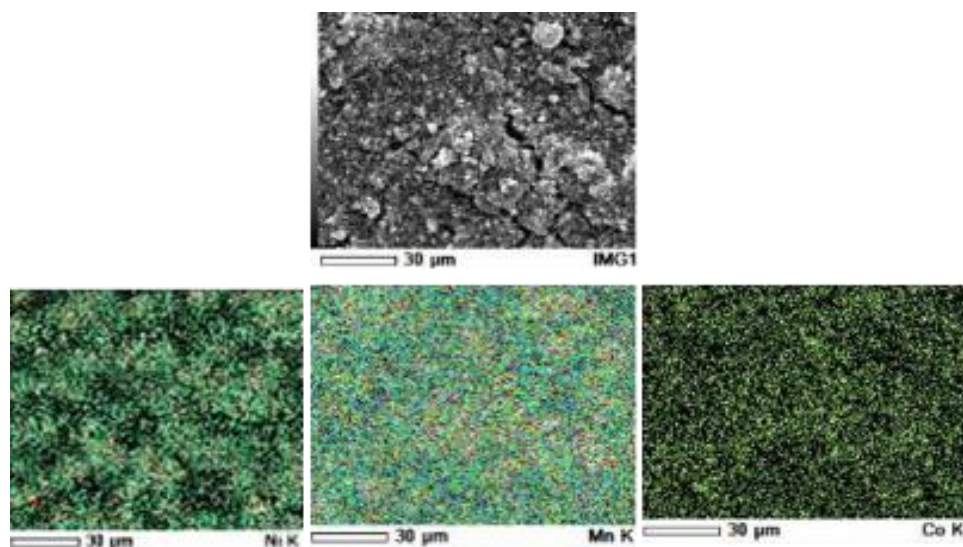


Figure 12. Mapping the surface of NMC 111 cathode

higher conductivity. Further research is needed to optimize the coating conditions with AB and PVDF for other types of NMC. The findings of this study can serve as a reference for developing cathodes that offer optimal conductivity, thus improving battery performance, particularly for electric vehicles. However, this study is limited to the use of AB and PVDF additives on only NMC 111 and NMC 811 cathode materials, and further development is necessary to explore their application on NMC 541, a material with more challenging microstructural control.

Acknowledgments

Thanks to the Indonesian National Research and Innovation Agency (BRIN) and the Indonesian Nuclear Technology Polytechnic for

providing funding and testing facilities in this research.

Author's Declaration

Authors' contributions and responsibilities

TD: Initiating the research idea and activities, Determining the research methodology, Analyzing Data, Monitoring and evaluating the research; **AS:** a. Preparing research materials, Creating test samples; **EY:** Assisting in analyzing experimental data, Collecting data and references; **S:** a. Preparing machinery and equipment for sample production, Assisting in sample production; **YP:** Assisting in analyzing experimental results, Assisting in monitoring and evaluating the research; **BS:** Preparing samples for SEM testing, Conducting SEM testing; **IAPW:** Preparing samples for conductivity testing, Conducting conductivity testing.

Funding

National Research and Innovation Agency (BRIN) and Indonesian Nuclear Technology Polytechnic.

Availability of data and materials

All data are available from the authors.

Competing interests

The authors declare no competing interest.

Additional information

No additional information from the authors.

References

- [1] M. Noga, P. Gorczyca, and R. Hebda, "The Effects of Use of the Range Extender in a Small Commercial Electric Vehicle," *Automotive Experiences*, vol. 4, no. 1, pp. 5–19, 2021, doi: 10.31603/ae.4137.
- [2] A. Krisbudiman *et al.*, "Structural Design Analysis Torque Links of Nose Landing Gear on Light Aircraft," *International Journal on Advanced Science, Engineering and Information Technology*, vol. 14, no. 2, pp. 507–513, 2024, doi: 10.18517/ijaseit.14.2.19317.
- [3] J. E. Dakurah, H. Solmaz, and T. Kocakulak, "Modeling of a PEM Fuel Cell Electric Bus with MATLAB/Simulink," *Automotive Experiences*, vol. 7, no. 2, pp. 252–269, Sep. 2024, doi: 10.31603/ae.11471.
- [4] I. C. Setiawan and M. Setiyo, "Fueling the Future: The Case for Heavy-Duty Fuel Cell Electric Vehicles in Sustainable Transportation," *Automotive Experiences*, vol. 7, no. 1, pp. 1–5, 2024, doi: 10.31603/ae.11285.
- [5] A. R. Abrari, T. H. Ariwibowo, D. Pramadihanto, N. R. Arini, E. H. Binugroho, and A. Miyara, "Thermal Performance Enhancement of Serpentine Cooling Design Using Branch Modification for Lithium-Ion Batteries," *Automotive Experiences*, vol. 6, no. 2, pp. 303–319, 2023, doi: 10.31603/ae.12709.
- [6] H. Maghfiroh, O. Wahyunggoro, and A. I. Cahyadi, "Low Pass Filter as Energy Management for Hybrid Energy Storage of Electric Vehicle: A Survey," *Automotive Experiences*, vol. 6, no. 3, pp. 466–484, 2023, doi: 10.31603/ae.9398.
- [7] Y. Guo *et al.*, "A high-voltage and low-solvating electrolyte towards promising micro-Si/Ni-rich NMC full cells," *Energy Storage Materials*, vol. 67, no. November 2023, p. 103258, 2024, doi: 10.1016/j.ensm.2024.103258.
- [8] O. Popović, V. Rugar, Ž. Praštalo, S. Aleksandrović, and V. Milisavljević, "Testing of NMC and LFP Li-ION cells for surface temperature at various conditions," *Case Studies in Thermal Engineering*, vol. 61, no. August, p. 104930, 2024, doi: 10.1016/j.csite.2024.104930.
- [9] M. Fakhruddin, E. Kartini, and A. Zulfia, "Microelectronic Engineering Improving performance of cathode NMC-811 by CeO₂ coating for Li-ion battery," *Microelectronic Engineering*, vol. 288, no. June 2023, p. 112169, 2024, doi: 10.1016/j.mee.2024.112169.
- [10] G. Mehmet, "Electrochimica Acta Synthesis of Sn-doped Li-rich NMC as a cathode material for Li-ion batteries," vol. 440, no. October 2022, pp. 1–9, 2023, doi: 10.1016/j.electacta.2022.141743.
- [11] H. Darjazi, E. Gonzalo, B. Acebedo, R. Cid, M. Zarrabeitia, and F. Bonilla, "Materials Today Sustainability Improving high-voltage cycling performance of nickel-rich NMC layered oxide cathodes for rechargeable lithium ion batteries by Mg and Zr co-doping," vol. 20, 2022, doi: 10.1016/j.mtsust.2022.100236.
- [12] Y. D. Herlambang *et al.*, "Study on Solar Powered Electric Vehicle with Thermal Management Systems on the Electrical Device Performance," *Automotive Experiences*, vol. 7, no. 1, pp. 18–27, 2024, doi: 10.31603/ae.10506.
- [13] Y. Liu *et al.*, "Toward scale-up of solid-state battery via dry electrode technology," *Next Energy*, vol. 7, no. July 2024, p. 100221, 2025, doi: 10.1016/j.nxener.2024.100221.
- [14] F. Han *et al.*, "Alkali-enhanced polyvinylidene fluoride cracking to deeply remove aluminum impurities for regeneration of battery-grade lithium iron phosphate," *Chemical Engineering Journal*, vol. 483, no. October 2023, p. 148973, 2024, doi: 10.1016/j.cej.2024.148973.
- [15] J. Kang, M. Atwair, I. Nam, and C. J. Lee, "Experimental and numerical investigation on effects of thickness of NCM622 cathode in Li-ion batteries for high energy and power density," *Energy*, vol. 263, no. PE, p. 125801, 2023, doi: 10.1016/j.energy.2022.125801.
- [16] Y. J. Song, J. Wang, and L. H. Liang, "Thickness effect on the mechanical performance of cathodes in lithium-ion

- batteries," *Journal of Energy Storage*, vol. 86, no. PB, p. 111417, 2024, doi: 10.1016/j.est.2024.111417.
- [17] R. Yang *et al.*, "Grain-refining Co_{0.85}Se@CNT cathode catalyst with promoted Li₂O₂ growth kinetics for lithium-oxygen batteries," *Chinese Chemical Letters*, vol. 35, no. 12, p. 109595, 2024, doi: 10.1016/j.ccllet.2024.109595.
- [18] J. Smekens *et al.*, "Influence of electrode density on the performance of Li-ion batteries: Experimental and simulation results," *Energies*, vol. 9, no. 2, pp. 1–12, 2016, doi: 10.3390/en9020104.
- [19] E. Yulianto and V. Mizeikis, "Autofocusing on direct laser writing techniques in photoresist using photoluminescence analysis," *AIP Conference Proceedings*, vol. 2561, p. 030002, 2022, doi: 10.1063/5.0112034.
- [20] E. Yulianto, M. Ningsih, W. Bahari, T. Maftukhah, and A. Musthofa, "Raman Spectroscopy for Non-Destructive Detection of Pesticide on Guava Peel," vol. 9, no. 4, pp. 2025–2029, 2025, doi: 10.29303/jppipa.v9i4.3202.
- [21] H. Widiyandari, R. A. Latifah, A. Jumari, C. S. Yudha, and Shofirul Sholikhatun Nisa, "Sintesis Material Katoda LiNi 0,8 Mn 0,1 Co 0,1 O₂ (NMC811) dengan Metode Solid State Menggunakan Nikel Hasil Perolehan Kembali dari Spent Nickel Catalyst," *ALCHEMY Jurnal Penelitian Kimia*, vol. 18, no. 2, pp. 214–220, 2022, doi: 10.20961/alchemy.18.2.63035.214-220.
- [22] Y. Liu, X. Wan, and J. Zheng, "Na/W co-doping enhances the electrochemical performance of Li-rich Mn-based cathode through improved electronic conductivity and promoted cationic migration," *Ceramics International*, vol. 50, no. 4, pp. 6289–6298, 2024, doi: 10.1016/j.ceramint.2023.11.357.